Crystal structure of $HgBa_2Ca_2Cu_3O_{8+\delta}$ at high pressure (to 8.5 GPa) determined by powder neutron diffraction

A. R. Armstrong and W. I. F. David
ISIS Facility, Rutherford Appleton Laboratory, Chilton, Didcot, Oxfordshire, OX11 0QX, United Kingdom

I. Gameson and P. P. Edwards*
School of Chemistry, University of Birmingham, Edgbaston, Birmingham, B15 2TT, United Kingdom

J. J. Capponi, P. Bordet, and M. Marezio*
Laboratoire de Cristallographie, CNRS, UJF Boîte Postale 166, 38042 Grenoble Cedex 09, France
(Received 27 January 1995)

The crystal structure of the high-temperature superconductor $HgBa_2Ca_2Cu_3O_{8+\delta}$ has been determined from powder neutron-diffraction experiments up to pressures of 8.5 GPa. Complete structural refinements were carried out on the experimental data taken at (approximate) pressures of <0.5, 3.5, 6.0, and 8.5 GPa. One of the most significant features to emerge from this study is the extreme sensitivity of the apical Cu-O bond to applied pressure. Between our ambient and high-pressure measurements the apical Cu-O bond length decreases by some 10.5%. In contrast, over the same pressure range, we have recorded significantly smaller changes in other crystal bond lengths. For example, the Cu-O in-plane bond distance changes by only around 2% as does the Hg-O apical bond. The availability of such structural data for this highest transition temperature superconductor may now allow an appraisal of the various structural and electronic factors responsible for superconductivity at such exceptionally high temperatures.

I. INTRODUCTION

The recent discoveries of superconductivity in the mercury-bearing cuprates has attracted considerable interest.[1–9] For the homologous series $HgBa_2Ca_{n-1}Cu_nO_{2n+2+\delta}$, this has led to record high superconducting transition temperatures (T_c). For $HgBa_2Ca_2Cu_3O_{8+\delta}$ (i.e., $n=3$) this temperature is now 135 K at ambient pressure[4] and 164 K under applied pressure.[9] Such remarkable advances illustrate, once again, that the upper limit to T_c in cuprate materials may not yet have been achieved. The structure of $HgBa_2Ca_2Cu_3O_{8+\delta}$ (shown in Fig. 1) is based on the complex layer sequence

$$\ldots(BaO)(HgO_\delta)(BaO)(CuO_2)Ca(CuO_2)Ca(CuO_2)(BaO)\ldots$$

in which rocksalt blocks of $(BaO)(HgO_\delta)(BaO)$ alternate with oxygen-deficient perovskite-like $(CuO_2)Ca(CuO_2)$ blocks.

Recent experiments have shown that the transition temperature of $HgBa_2Ca_2Cu_3O_{8+\delta}$ increases dramatically with the application of hydrostatic pressure, reaching a maximum value of 164 K at 31 GPA;[7–9] this represents a record value for T_c in any kind of environment, and a temperature only ~ 20 K below the lowest recorded ground temperature on this planet. Such high-pressure studies may provide vital information as to the possibility of superconductivity at yet higher temperatures. A major experimental goal would be to simulate such crystal-chemical pressure by appropriate synthesis and chemical substitutions under ambient pressure conditions. With these factors in mind we have undertaken an *in situ* structural determination of $HgBa_2Ca_2Cu_3O_{8+\delta}$ (Hg1223) up to pressures of 8.5 GPa using powder neutron diffraction on the high intensity, medium resolution POLARIS diffractometer at the Rutherford Appleton Laboratory.[10]

II. EXPERIMENTAL

A. Synthesis

Samples of $HgBa_2Ca_2Cu_3O_{8+\delta}$ were prepared using the method described in Ref. 11. A mixed precursor with the nominal composition $Ba_2Ca_2Cu_3O_x$ was prepared from a

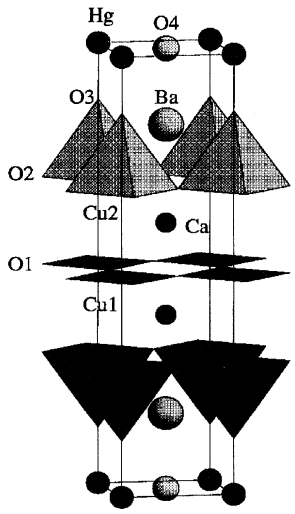

FIG. 1. A schematic representation of the structure of $HgBa_2Ca_2Cu_3O_{8+\delta}$.

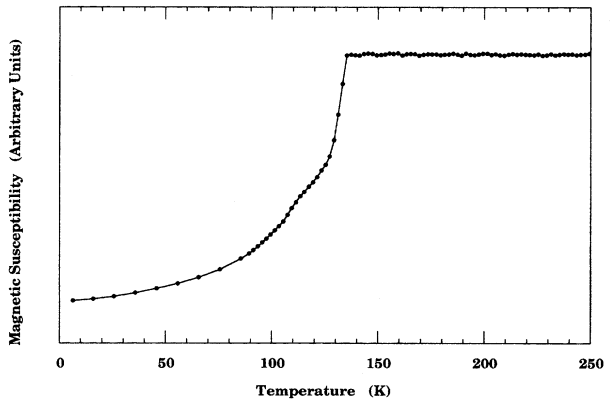

FIG. 2. Magnetic susceptibility of $HgBa_2Ca_2Cu_3O_{8+\delta}$ showing T_c to be between 134 and 135 K.

stoichiometric mixture of the component nitrates under flowing oxygen at 925 °C for 72 h with three intermediate grindings. A stoichiometric amount of yellow HgO was added to this precursor and the mixture placed in a gold capsule adapted for high pressure synthesis. The sample was pressurized to 1.8 GPa over the course of 20 min and then heated to 880 °C in 40 min. The temperature and pressure were then maintained or 1.6 to 1.8 h before switching the furnace off and decreasing the pressure to ambient over a period of 20 min.

B. Magnetic characterization

Superconducting properties were measured using a dc superconducting quantum interference device magnetometer (Cryogenics Model S100); here the sample vial was lowered into the cryostat and cooled to ~4 K in the absence of any externally generated magnetic field (Fig. 2).

C. Neutron diffraction

Time-of-flight powder neutron-diffraction measurements were performed on the high intensity, medium resolution POLARIS diffractometer at the ISIS facility at the Rutherford Appleton Laboratory.[10] An ambient pressure measurement was made in a cylindrical vanadium can to obtain accurate starting parameters for the refinement of the high-pressure data. Since mercury is a relatively strong absorber ($\sigma_a = 372.3$ b) these ambient data were corrected for sample attenuation. High-pressure measurements were made using the Paris Edinburgh opposed anvil pressure cell with a sample volume of ~100 mm^3. Details of this cell are given elsewhere[12] but using tungsten carbide anvils a maximum pressure of around 10.0 GPa can be achieved. High-pressure diffraction data were collected using the detector bands at scattering angles of $82° < 2\theta < 96°$, which gives data over the d spacing range $0.3 < d < 4.3$ Å with a resolution of $\Delta d/d \sim 0.6\%$. Each data set was collected over a period of 12–15 h. The data were normalized to remove the wavelength dependence of the incident neutron flux and corrected for the effects of attenuation of the incident and scattered beams by components of the pressure cell. Data sets were obtained at applied loads of 20, 65, 85, and 110 tonnes corresponding to approximate pressures of <0.5, 3.5, 6.0, and 8.5 GPa. Unfortunately constraints of time prevented an equation-of-state experiment from being carried out and these applied pressures have been inferred from the applied load given the known behavior of the pressure cell for similar materials. (Hence the rather large errors shown in the figures.) In an earlier neutron-diffraction study by Hunter *et al.*[17] one of the impurity phases (CaO) was used as an internal pressure calibration to determine the actual sample pressure. Such an approach cannot be applied here however due to the lack of CaO in our samples. Nevertheless it is possible to use the bulk modulus determined by Hunter *et al.*[17] in combination with our measured changes in unit-cell volume to calibrate our pressure readings. Unfortunately their bulk modulus was determined from only two pressure readings and such a calibration results in a linear dependence of the lattice constants with pressure. This we feel is unreasonable and hence we have continued to use the pressure readings inferred from the applied load.

TABLE I. Final refined parameters at ambient pressure for $HgBa_2Ca_2Cu_3O_{8+\delta}$ and $HgBa_2Ca_3Cu_4O_{10+\delta}$.

		Hg1223	Hg1234
a/Å		3.85159(3)	3.85159(3)
c/Å		15.7644(4)	18.9919(12)
Hg	B_{iso}	1.66(6)	1.66(6)
Ba	z	0.1696(4)	0.1487(13)
	B_{iso}	0.30(7)	0.30(7)
Ca(1)	z	0.3950(5)	0.3298(12)
	B_{iso}	0.30(5)	0.30(5)
Ca(2)	B_{iso}		0.30(5)
Cu(1)	z	0.5	0.4183(7)
	B_{iso}	0.45(10)	0.04(4)
Cu(2)	z	0.2986(3)	0.2479(7)
	B_{iso}	0.04(4)	0.04(4)
O(1)	z	0.5	0.4217(7)
	B_{iso}	0.35(8)	0.28(4)
O(2)	z	0.3014(3)	0.2445(7)
	B_{iso}	0.28(4)	0.28(4)
O(3)	z	0.1256(4)	0.1090(11)
	B_{iso}	0.54(6)	0.54(6)
O(4)	B_{iso}	0.5	0.5
	n	0.16(3)	0.55(10)

The ambient pressure structure of Hg1223 was refined using the program TF14LS based on the Cambridge Crystallographic Subroutine Library,[13,14] using the model of Chmaissem *et al.* but without splitting the Ba site.[11] Scattering lengths of 1.2692, 0.507, 0.476, 0.7718, and 0.5803 (all $\times 10^{-12}$ cm) were assigned to Hg, Ba, Ca, Cu, and O, respectively.[15] A number of reflections arising from impurities in the sample were observed, the most significant of which came from $HgBa_2Ca_3Cu_4O_{10+\delta}$ (Hg1234). Other impurity phases such as "$BaCuO_2$" and $CaHgO_2$ which are present in only small quantities were also included as test of the refinement. In this context we were conscious of the observation of Hunter *et al.*[17] that the O(3) z coordinate is sensitive to the treatment of impurity phases. The inclusion of these two minor phases however had no marked effect on the

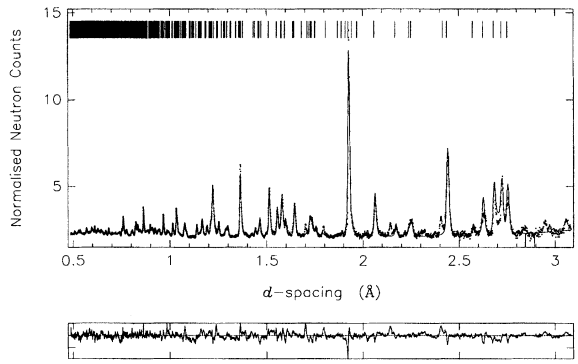

FIG. 3. The profile fit for $HgBa_2Ca_2Cu_3O_{8+\delta}$ at ambient pressure. The allowed reflections from Hg1223 are shown; the profile fit also includes the $HgBa_2Ca_3Cu_4O_{10+\delta}$ phase.

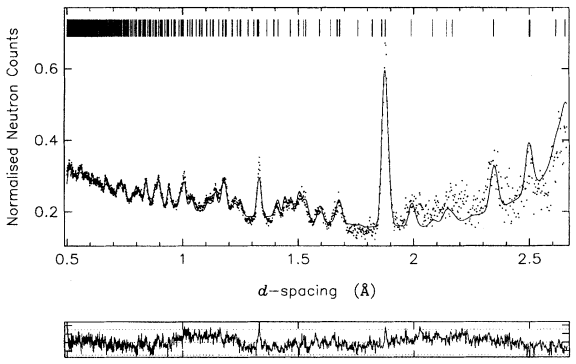

FIG. 4. The profile fit for $HgBa_2Ca_2Cu_3O_{8+\delta}$ at 8.5 GPa pressure. The allowed reflections for the Hg1223 phase are indicated.

outcome of the refinements. In order to simplify our model from four to two phase these minor impurities were not included in subsequent refinement. As a result two phase refinement was performed using the program FORTY1, also based on the Cambridge Crystallographic Subroutine Library. All positional parameters were refined, along with isotropic thermal parameters for all atoms except O(4) in the Hg planes. Thermal parameters for similar sites in Hg1223 and Hg1234 were constrained to be equal.

The high-pressure data was also refined using FORTY1, but in addition to these two phases, parameters for tungsten carbide from the anvils of the pressure cell were refined. Since the number of clearly identifiable peaks in the high-pressure data arising from Hg1234 are small, the a lattice parameter was constrained to be the same as that of Hg1223. The c lattice parameter was deduced from the compressibility of Hg1223 with the addition of the compressibility of an additional $CaCuO_2$ unit. An overall temperature factor covering both phases was refined, whilst individual atomic thermal parameters were fixed at the values obtained from the ambient pressure and temperature data. The atomic positional parameters for Hg1223 were varied whilst changes in those for Hg1234 were deduced from those of its three-layer counterpart.

III. RESULTS AND DISCUSSION

A. Ambient pressure structure

Rietveld analysis of the ambient pressure data converged smoothly for both the single and two-phase refinements. Final refined parameters for both Hg1223 and Hg1234 phases are given in Table I and the profile fit to the data is shown in Fig. 3. Note that in Fig. 3 the allowed reflections for Hg1223 are indicated, but the complete profile fit includes both the Hg1223 and Hg1234 phases.

The values for Hg1223 are in good agreement with those of an earlier powder neutron-diffraction study[11] and also a recent single crystal structure determination.[16] These values were used as the starting point for the refinement of the data obtained in the high-pressure cell.

B. The effect of pressure

Table II shows the refined lattice constants and atomic z coordinates for Hg1223 under the different loadings. The profile fit for the 8.5 GPa data is shown in Fig. 4.

1. Cell constants

Figure 5 shows the effect of hydrostatic pressure on the lattice constants of Hg1223. The decrease in both a and c is essentially linear with $da/dP \sim -0.011$ Å/GPa and $dc/dP \sim -0.090$ Å/GPa; with some deviation from linearity at the highest applied pressures; note that the decrease of the c parameter is ~ 8 times that of the a parameter. Hunter *et al.* [17] have reported a high-pressure neutron diffraction study of $HgBa_2CuO_{4+\delta}$ (Hg1201), $HgBa_2CaCu_2O_{6+\delta}$ (Hg1212), and Hg1223. There are slight differences in the lattice constants from the present work and that of Hunter *et al.* ($\Delta a = 0.0056$ Å, $\Delta c = 0.0086$ Å). However, we feel that such small differences are well within the systematic errors limits for two independent studies. Both investigations

TABLE II. Final refined parameters for $HgBa_2Ca_2Cu_3O_{8+\delta}$ at various pressures.

	Applied pressure (GPa)				
	0	0.5	3.5	6.0	8.5
a/Å	3.85159(3)	3.8481(2)	3.8089(3)	3.7822(5)	3.7608(6)
c/Å	15.7644(4)	15.740(3)	15.400(4)	15.180(6)	15.018(7)
Baz	0.1696(4)	0.1678(9)	0.1674(12)	0.1661(12)	0.1651(13)
Caz	0.3950(5)	0.3950(12)	0.3999(15)	0.3965(17)	0.3931(16)
Cu(2)z	0.2986(3)	0.2973(6)	0.2963(9)	0.2964(10)	0.2934(9)
O(2)z	0.3014(3)	0.3029(7)	0.3015(9)	0.2997(10)	0.3003(10)
O(3)z	0.1256(4)	0.1256(7)	0.1265(10)	0.1271(12)	0.1309(13)

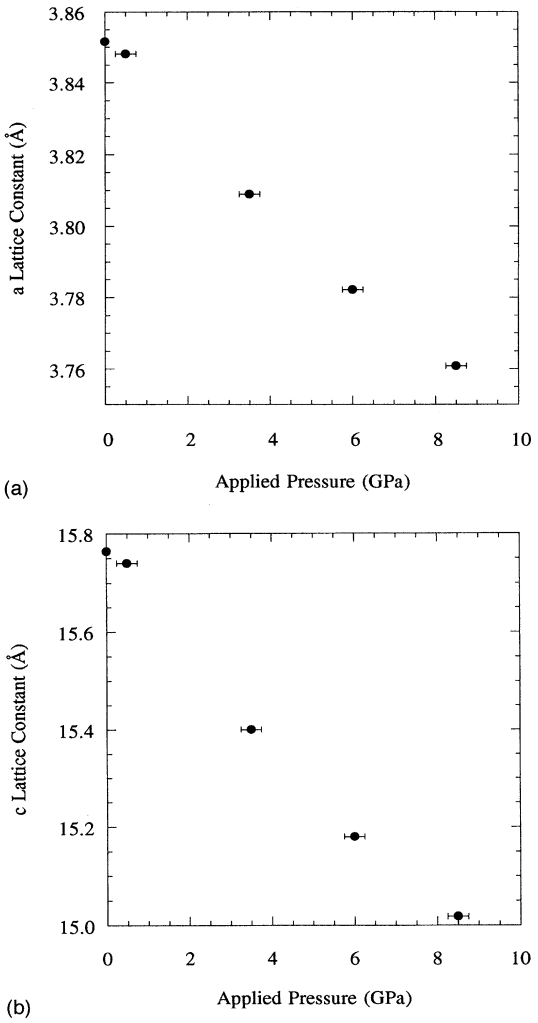

FIG. 5. The a and c lattice constants of $HgBa_2Ca_2Cu_3O_{8+\delta}$ at various applied pressures.

are on samples having the maximum T_c of 135 K (see Fig. 2), suggesting that the oxygen contents are essentially the same.

2. Compressibility of cell constants

The compressibility κ of a structural parameter m is given by $\kappa_m = -(1/m)[\partial m(P)/\partial P]$. Hence from the unit-cell data is possible to calculate the compressibility along the a and c axes as well as the overall unit-cell volume (κ_a, κ_c, and κ_v, respectively). This in turn yields the bulk modulus (B) of the structure via the relationship $B = 1/\kappa_v$. The values of these compressibility parameters are listed in Table III. In addition to our experimental results of those of Hunter *et al.* [17] the results of two theoretical studies on this system are also included.[18,19]

The results of Cornelius and Schilling[18] are derived using a model based on the ideas of comparative crystal chemistry.[20] Novikov, Mryasov, and Freeman[19] have performed local-density approximation calculations to investigate the effects of pressure on the single CuO_2 layer Hg1201

TABLE III. Compressibilities of the lattice constants κ_m (in units of 10^{-3}/GPa), bulk modulus B (GPa), and anisotropy parameter (κ_c/κ_a) for $HgBa_2Ca_2Cu_3O_{8+\delta}$.

	κ_a	κ_c	κ_v	B	κ_c/κ_a	Ref.
Experimental	2.82	5.72	11.1	90	2.03	This work
	2.57	5.62	10.8	93	2.18	17
	2.28	4.7	9.1	110	2.07	17 [a]
Calculated	2.9	4.0	9.9	101	1.38	18
	2.54	4.37	9.45	106	1.72	19

[a]Results determined from Hunter *et al.* (Ref. 17) using structural parameters at 0, 4.0, and 9.2 GPa only.

structure and also the infinite layer (IL) $(Sr_{1-x}Ca_x)_{1-y}CuO_2$ material. These authors considered the structure of the double, triple, and quadruple CuO_2 layer Hg materials as simple combinations of Hg1201 and IL blocks and subsequently arrives at the figures reported in Table III.

The anisotropic nature of the compressibility (as expressed by κ_c/κ_a) is clearly evident from the data given in Table III. Whilst there is general agreement between the experimentally determined values of κ_a and κ_c, the results from the theoretical models show consistently smaller values of κ_c. Hence the predicted anisotropy parameter is smaller than the experimentally determined value. It seems clear from these results that dividing the Hg1223 structure into subunits for which compressibility parameters are already known and using these known values to predict the effect of pressure on the three-layer Hg phase is perhaps something of an over simplification. With the availability of data for a number of Hg-containing cuprates, it would now seem appropriate to look in more detail at these calculations.

3. Bond lengths

The effect of pressure on the individual bond lengths can be seen in Table IV and the changes in selective Cu-O, Hg-O, and Ba-O bonds are shown in Figs. 6–8, respectively. It should be noted that the variations in Cu(1)-O(1) distances are virtually identical to those of Cu(2)-O(2) and, as such, only the changes in Cu(2)-O(2) are shown in the figure.

At ambient pressure the Cu(2)O(3) apical bond distance is extremely large (2.727 Å) and the results of the refinement shows that this decreases by 10.5% (to 2.440 Å) on going to 8.5 GPa. Note that this decrease in the Cu(2)-O(3) apical bond corresponds to 38% of the total decrease of the c lattice constant. Equally impressive is the insensitivity of the Hg-O(3) apical distance to pressure (0.014 Å decrease over the same pressure range, 2% of the c-axis contraction) as this also lies entirely along the c axis. The picture that emerges is that of a highly compressible Cu(2)-O(3) bond and a virtually incompressible Hg-O(3) bond (see below).

The large compression of the Cu(2)-O(3) apical bond contrasts sharply with the 2.2% decrease (1.926 to 1.883 Å) in the Cu(2)-O(2) in-plane distance over the same pressure range. The consistently small changes (2.2–2.4 %) in all the in-plane bonds [Hg-O(4), Cu(1)-O(1), and Cu(2)-O(2)] is the source of the small contraction of the a lattice parameter (Figs. 6 and 7).

TABLE IV. Bond lengths for $HgBa_2Ca_2Cu_3O_{8+\delta}$ at various pressures.

	Applied pressure (GPa)				
	0	0.5	3.5	6.0	8.5
Hg-O(3)	1.980(6)	1.977(12)	1.948(16)	1.929(18)	1.966(20)
Hg-O(4)	2.723(7)	2.721(18)	2.693(25)	2.674(28)	2.659(30)
Cu(2)-O(3)	2.727(7)	2.703(17)	2.613(23)	2.570(26)	2.440(27)
Cu(1)-O(1)	1.926(1)	1.924(1)	1.905(1)	1.891(1)	1.880(1)
Cu(2)-O(2)	1.926(5)	1.926(11)	1.906(15)	1.892(17)	1.883(18)
Cu(1)-Cu(1)	3.175(4)	3.190(11)	3.130(13)	3.091(15)	3.103(14)
O(1)-O(2)	3.131(5)	3.102(11)	3.057(14)	3.041(15)	2.999(15)
Ba-O(2)	2.833(8)	2.868(18)	2.809(21)	2.773(23)	2.767(23)
Ba-O(3)	2.810(9)	2.801(18)	2.766(24)	2.739(26)	2.708(26)
Ba-O(4)	2.674(6)	2.641(15)	2.578(18)	2.521(19)	2.479(19)
Ca-O(1)	2.539(8)	2.536(20)	2.450(23)	2.459(26)	2.473(24)
Ca-O(2)	2.426(10)	2.409(25)	2.434(29)	2.395(33)	2.341(31)

4. Compressibility of chemical bonds

The compressibility of all the bonds listed in Table IV have been calculated and a selected number of these are shown in Table V. In addition, data for Hg1201 and Hg1212 (Ref. 17) have been included. It might be anticipated that under applied pressure cation-anion interaction will have a higher compressibility than anion-anion and cation-cation interactions. An examination of the Hg1223 structure shows that the major cation-anion interactions along the c axis are the Hg-O(3) and Cu(2)-O(3) bonds, i.e., the cation-apical oxygen bonds. The remaining major interactions are likely to be Cu(2)-Cu(1) cation-cation repulsions but other bonds will, of course, have small components along the c axis.

Hunter *et al.* [17] found that for the single and double CuO_2 layer compounds the Cu-apical O bond has a compressibility greater than κ_c but that the Hg-apical O bond is virtually unchanged. In contrast, for the triple CuO_2 layer compound they reported the reverse trend, vis. the Cu(2)-O(3) bond was not strongly compressible. This result is very surprising considering the fact that the Cu(2)-O(3) distance is some 0.7 Å longer than the Hg-O(3) bond. In contrast, we find a highly compressible Cu(2)-O(3) bond for $HgBa_2Ca_2Cu_3O_{8+\delta}$.

Figures 6 and 7 show that applied pressure has very little effect on the Hg-O(3) bond in contrast to a significant contraction of the Cu(2)-O(3) bond. This is consistent with the results[17] from the single and double CuO_2 layer Hg phase and is reflected in the compressibility values given in Table V for the various chemical bonds in the single, double, and triple CuO_2 layer mercury cuprates.

IV. CONCLUDING REMARKS

The most prominent feature to emerge from these experiments on $HgBa_2Ca_2Cu_3O_{8+\delta}$ is the drastic shortening of the apical Cu-O bond with pressure; the Cu(2)-O(3) bond length changes from 2.727 Å at ambient pressure to 2.440 Å at 8.5 GPa, a change of some 10.5%. Over the same pressure range the Cu(2)-O(2) in-plane distance, for example, decreases by only 2.2% while the Hg-O(3) apical distance reduces also by

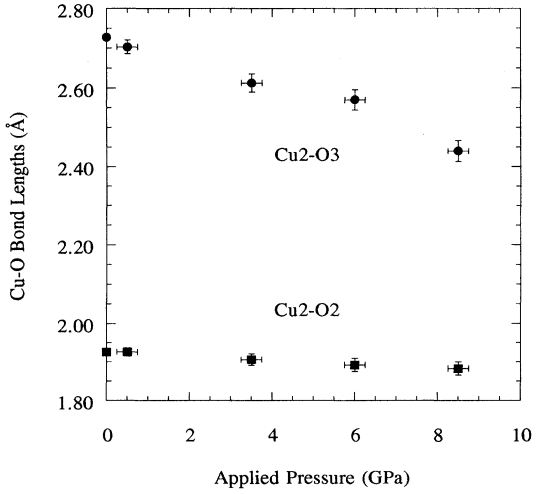

FIG. 6. Copper-oxygen distances versus applied pressure for $HgBa_2Ca_2Cu_3O_{8+\delta}$. See Fig. 1 for nomenclature.

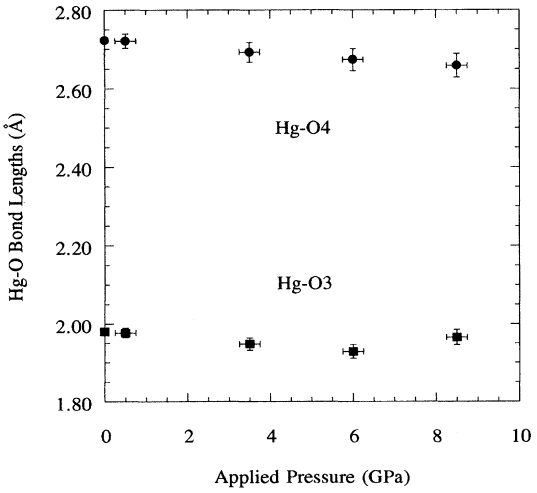

FIG. 7. Mercury-oxygen distances versus applied pressure for $HgBa_2Ca_2Cu_3O_{8+\delta}$. See Fig. 1 for nomenclature.

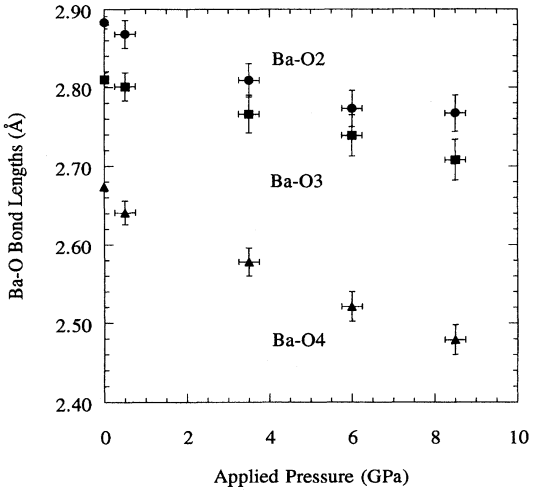

FIG. 8. Barium-oxygen distances versus applied pressure for $HgBa_2Ca_2Cu_3O_{8+\delta}$. See Fig. 1 for nomenclature.

only 2%. The da/dP and dc/dP coefficients also illustrate that the crystal compressibility is highly anisotropic.

From a structural point of view, the arrangement of the superconducting and charge reservoir blocks in $HgBa_2Ca_2Cu_3O_{8+\delta}$ are somewhat similar to those found in $YBa_2Cu_3O_{7+\delta}$.[21] Thus, the structure contains blocks such as $(CuO_2)(BaO)(HgO_\delta)(BaO)(CuO_2)$ or $(CuO_2)(BaO)(CuO_\delta)(BaO)(CuO_2)$ in which (CuO_2) is the (common) superconducting layer and (HgO_δ) and (CuO_δ) are the corresponding charge reservoirs. At this stage, it seems reasonable that the very different pressure effects for the Hg-bearing cuprates and $YBa_2Cu_3O_{7+\delta}$ may arise from the differences in the coordination chemistry of the apical oxygens. In $YBa_2Cu_3O_{7+\delta}$ the apical is coordinated to two Cu cations, whereas in $HgBa_2Ca_2Cu_3O_{8+\delta}$ one finds the apical oxygen bound to a copper cation and a Hg cation. The characteristic dumb bell bond between Hg and O(3) is only 1.980 Å at ambient pressure whereas the Cu(2)-O(3) apical bond is exceptionally long at 2.727 Å; indeed this Cu-O distance might lead one to question the appellation "chemical bond." This situation almost certainly ensures that the Cu-O-Hg bond is highly compressible while the Cu-O-Cu bond in $YBa_2Cu_3O_{7+\delta}$ is only marginally compressible.

It is widely noted that this structural parameter is intimately related to the nature of the electronic band structure of the superconducting cuprates. In particular, the energy

TABLE V. Compressibilities of selected chemical bonds (in units of 10^{-3}/GPa).

Compressibilities	Hg1201 [a]	Hg1212 [a]	Hg1223 [a, b]	Hg1223 [c]
$\kappa_{Cu(2)-O(3)}$	9(3)	14(4)	2(2)	11(2)
$\kappa_{Hg-O(3)}$	1(4)	0(4)	14(2)	2(1)
κ_{Cu-Cu}		0(2)	1(1)	3(1)
$\kappa_{interlayer}$	6(1)	8(2)	7(7)	7(2)

[a]Taken from Hunter *et al.* (Ref. 17).
[b]Results determined using structural parameters at 0, 4.0, and 9.2 GPa only.
[c]This work.

level of the apical oxygen ions have been shown to play a fundamental role in the control of the electronic structure of the CuO_2 planes, most notably in governing the maximum value of T_c.[22–24] While the dramatic effect of pressure on T_c and the apical Cu-O bond may be shown to be closely interrelated, it is important to recognize, and take account of, the totality of crystal structure changes under hydrostatic pressure. As just one example, we note that Novikov and Freeman[25] have discussed the influence of Ca ions situated between the CuO_2 layers on the electronic energy bands of these systems. Here an indirect interaction involving Ba $(2p)$ states effects the energy of the HgO band. The downward movement of the Hg band charge reservoir electronic band–and hence the degree of charge transfer–is caused by the subtle interplay between the Ca $(4p)$ and Ba $(2p)$ states that ultimately govern its location in relation to the Cu $(3d)$-O$(2p)$ states.[25] Such features are also highlighted by Rodriguez, Christensen, and Peltzer y Blanca.[26] The present determination of the crystal structure of $HgBa_2Ca_2Cu_3O_{8+\delta}$ at various high pressures may now allow a more complete evaluation of the structural and electronic features responsible for superconductivity at such exceptionally high temperatures.

ACKNOWLEDGMENTS

We are very grateful to S. Hull, S. Klotz, J. S. Loveday, R. J. Nelmes, and M. Slaski for assistance and discussions and A. D. Taylor for the award of discretionary time at the ISIS facility. We also thank EPSRC for financial support and acknowledge that this collaboration was made possible through the Basic Espirit Program, Working Group 6885 HTSC.

*Correspondence to be sent to Professor P. P. Edwards, School of Chemistry, University of Birmingham, Edgbaston, Birmingham. B15 2TT, England.

[1] R. S. Liu, S. F. Hu, D. A. Jefferson, P. P. Edwards, and P. D. Hunneyball, Physica C **205**, 206 (1993).
[2] S. F. Hu, D. A. Jefferson, R. S. Liu, and P. P. Edwards, J. Solid State Chem. **103**, 280 (1993).
[3] S. N. Putlin, E. V. Antipov, O. Chmaissem, and M. Marezio, Nature (London) **362**, 226 (1993).
[4] A. Schilling, M. Cantoni, J. D. Guo, and H. R. Ott, Nature (London) **363**, 56 (1993).
[5] S. N. Putlin, E. V. Antipov, and M. Marezio, Physica C **212**, 266 (1993).
[6] E. V. Antipov, S. M. Loureiro, C. Chaillout, J. J. Capponi, P. Bordet, J. L. Tholence, S. N. Putlin, and M. Marezio, Physica C **215**, 1 (1993).
[7] C. W. Chu, L. Gao, F. Chen, Z. J. Huang, R. L. Meng, and Y. Y. Zue, Nature (London) **365**, 323 (1993).
[8] M. Nunez-Regueiro, J. L. Tholence, E. V. Antipov, J. J. Capponi, and M. Marezio, Science **262**, 97 (1993).
[9] L. Gao, Y. Y. Xue, F. Chen, Q. Xiong, R. L. Meng, D. Ramirez, C.

W. Chu, J. J. Eggert, and H. K. Mao, Phys. Rev. B **50**, 4260 (1994).

[10] R. I. Smith, S. Hull, and A. R. Armstrong, Mater. Science Forum **166-169**, 251 (1994).

[11] O. Chmaissem, Q. Huang, E. V. Antipov, S. N. Putlin, M. Marezio, S. M. Loureiro, J. J. Capponi, J. L. Tholence, and A. Santoro, Physica C **217**, 265 (1993).

[12] J. M. Besson, R. J. Nelmes, G. Hamel, J. S. Loveday, G. Weill, and S. Hull, Physica B **180-181**, 907 (1992).

[13] J. C. Matthewman, P. Thompson, and P. J. Brown, J. Appl Cyrstallogr. **15**, 167 (1982).

[14] P. J. Brown and J. C. Matthewman (unpublished).

[15] V. F. Sears, Neutron News **3** (3), 26 (1992).

[16] L. W. Finger, R. M. Hazen, R. T. Downs, R. L. Meng, and C. W. Chu, Physica C **226**, 216 (1994).

[17] B. A. Hunter, J. D. Jorgensen, J. L. Wagner, P. G. Radaelli, D. G. Hinks, H. Shaked, R. L. Hitterman, and R. B. Von Dreele, Physica C **221**, 1 (1994).

[18] A. L. Cornelius and J. S. Schilling, Physica C **218**, 369 (1993).

[19] D. L. Novikov, O. N. Mryasov, and A. J. Freeman, Physica C **222**, 38 (1994).

[20] R. M. Hazen and L. W. Finger, *Comparative Crystal Chemistry* (Wiley, New York, 1982).

[21] M. Marezio *et al.* (unpublished).

[22] See, for example, Y. Ohtu, T. Tohyamu, and S. Maekawa, Phys. Rev. B **43**, 2968 (1991), and references therein.

[23] K. A. Müller, Z. Phys. B **80**, 193 (1990).

[24] Kh. Eid, M. Matlak, and J. Zielinski, Physica C **220**, 61 (1994).

[25] D. L. Novikov and A. J. Freeman, Physica C **216**, 273 (1993).

[26] C. O. Rodriguez, N. E. Christensen, and E. L. Peltzer y Blanca, Physica C **216**, 12 (1993).